JOURNAL OF VIROLOGY, Sept. 1991, p. 4759–4768
0022-538X/91/094759-10$02.00/0

Vol. 65, No. 9

Neuropathological Changes in Scrapie and Alzheimer's Disease Are Associated with Increased Expression of Apolipoprotein E and Cathepsin D in Astrocytes

JANE F. DIEDRICH,[1] HAL MINNIGAN,[1] RICHARD I. CARP,[2] JOHN N. WHITAKER,[3] RICHARD RACE,[4] WILLIAM FREY II,[5] AND ASHLEY T. HAASE[1]*

Department of Microbiology, University of Minnesota, Minneapolis, Minnesota 55455[1]; Department of Virology, New York State Institute of Basic Research, Staten Island, New York 10314[2]; Department of Neurology, University of Alabama, Birmingham, Alabama 35294[3]; Laboratory of Persistent Viral Diseases, Rocky Mountain Laboratories, Hamilton, Montana 59840[4]; and Psychiatry Research Laboratories, St. Paul Ramsey Medical Center, St. Paul, Minnesota 55101[5]

Received 7 March 1991/Accepted 15 May 1991

With the rationale that the neuropathological similarities between scrapie and Alzheimer's disease reflect convergent pathological mechanisms involving altered gene expression, we set out to identify molecular events involved in both processes, using scrapie as a model to study the time course of these changes. We differentially screened a cDNA library constructed from scrapie-infected mice to identify mRNAs that increase or decrease during disease and discovered in this way two mRNAs that are increased in scrapie and Alzheimer's disease. These mRNAs were subsequently shown by sequence analysis to encode apolipoprotein E and cathepsin D (EC 3.4.23.5). Using in situ hybridization and immunocytochemistry to define the cellular and anatomic pathology of altered gene expression, we found that in both diseases the increase in apolipoprotein E and cathepsin D mRNAs and proteins occurred in activated astrocytes. In scrapie, the increase in gene expression occurred soon after the amyloid-forming abnormal isoform of the prion protein has been shown to accumulate in astrocytes. In Alzheimer's disease, the increased expression of cathepsin D also occurred in association with β-amyloid. These studies reveal some of the molecular antecedents of neuropathological changes in scrapie and Alzheimer's disease and accord new prominence to the role of astrocytes in neurodegenerative conditions.

Scrapie is a transmissible neurodegenerative disease of sheep and goats that is characterized by a long incubation period followed by a relentlessly progressive illness involving the central nervous system. While the progressive dementia in humans, Alzheimer's disease (AD), has not been proven to be transmissible, there are similarities in the central nervous system lesions in both conditions that include astrocytosis, amyloid deposition, vacuolation, neuron loss, and neuroaxonal dystrophy (31). These alterations have been extensively characterized by light and electron microscopy, but there is little understanding of their molecular basis. We have hypothesized that these similarities reflect convergent pathological mechanisms that at the molecular level involve activation or repression of a defined set of genes whose altered expression is responsible for the neurodegenerative changes (10, 21). In support of this hypothesis are the documented increases in glial fibrillary acidic protein (GFAP) (11, 38, 51), the B chain of α-crystallin, metallothionein II, and sulfated glycoprotein 2 (11a, 14, 15) in scrapie and AD.

In this study we have continued our search for changes in gene expression that occur in scrapie and AD by comparing mRNA populations in control and diseased brain tissues by differential screening of a cDNA library. We examined the spatial relationship of altered gene expression to neuropathological changes by mapping the mRNAs and proteins, using in situ hybridization and immunocytochemistry, and assessed the temporal relationship between altered gene expression and lesion development in longitudinal studies in a scrapie animal model. We found in this way that there are two mRNAs, apolipoprotein E (apoE) and cathepsin D (CD), that increase in abundance in both diseases and that the increase in gene expression maps to astrocytes associated with the neuropathological lesions. In scrapie this increased expression of genes in astrocytes preceded the other pathological manifestations of infection but followed the recently documented (12) accumulation in astrocytes of the major component of amyloid in scrapie, the abnormal isoform of the prion protein (PrP^{Sc}). In AD we found that the increase in CD was closely related spatially to classical β-amyloid-containing plaques. These studies implicate astrocytes in the formation or processing of amyloid proteins in the central nervous system and, more generally, sustain our confidence in the utility of this experimental approach in establishing the molecular and cellular correlates of pathological processes.

MATERIALS AND METHODS

Tissues. For RNA isolation, female weanling C57BL/6J mice (Jackson Laboratories, Bar Harbor, Maine) were injected intracerebrally with brain homogenate from mice infected with the 22L strain of the scrapie agent (C57BL/Scrapie) or with normal mouse brain homogenate (C57BL/Control) (28). Rocky Mountain Laboratory Swiss mice (Rocky Mountain Laboratories, Hamilton, Mont.) were injected intracerebrally with brain homogenate of mice infected with the Chandler strain of scrapie (RML Swiss/Scrapie) (22) or with normal mouse brain homogenate (RML Swiss/Control). The animals were killed by CO_2 asphyxiation during the late stage of clinical disease. Brains were

* Corresponding author.

removed as quickly as possible and placed at −70°C. Brain tissues from 5 to 10 animals were pooled for RNA isolation.

The human brain tissues for Northern (RNA) blot analyses were obtained from a 75-year-old male diagnosed with moderately severe AD (Alzheimer's) and a 63-year-old male without any evidence of AD, clinically or histologically (Aged). Pathological criteria for AD were based on the presence of moderate or severe neuritic plaques in the cortex, similar to accepted criteria (27). Slices of the frontal cortex were stored at −70°C for subsequent RNA isolation. Postmortem times were less than 5 h.

For in situ hybridization and immunocytochemistry studies, two groups of C57BL/6J mice were used. One group was injected intracerebrally with 22L mouse brain homogenate, and the second group was injected with normal mouse brain homogenate. One animal of each group was sacrificed at 4-week intervals beginning at 4 weeks postinoculation and ending at 20 weeks postinoculation. The approximate survival time for these animals was 22 weeks postinoculation (28). The mice were perfused with phosphate-buffered saline followed by freshly prepared 4% paraformaldehyde. The brains were removed and placed in 4% paraformaldehyde overnight before being transferred to 70% ethanol for storage at 4°C until they were embedded in paraffin. The brains were coded and examined "blindly." The code was not broken until the examinations were complete.

The human brain tissues for in situ hybridization and immunocytochemistry were obtained from four patients (ages 79 to 87 years) diagnosed with mild to moderately severe AD and from four patients (ages 53 to 69 years) that did not display any evidence of AD, clinically or histologically. Cubes of frontal or temporal cortex were placed in 10% neutral formalin for 7 to 48 h before being transferred to 70% ethanol at 4°C for storage until they were embedded in paraffin.

RNA isolation. The frozen tissue was homogenized in guanidium thiocyanate, and total RNA was isolated by sedimentation through cesium chloride as described by Chirgwin et al. (5). The poly(A)$^+$ RNA fraction was selected by two cycles of oligo(dT)-cellulose (Collaborative Research) chromatography (1, 32).

cDNA library construction. First-strand cDNA was synthesized from C57BL/Scrapie (16 weeks postinoculation) poly(A)$^+$ mRNA by reverse transcription with oligo(dT) primers. RNase H and *Escherichia coli* DNA polymerase I were used for synthesis of the second strand (20, 37), and T4 DNA polymerase was used to blunt the ends of the double-stranded cDNA (32). To prepare the double-stranded cDNA for ligation to the vector, it was methylated by *Eco*RI methylase (gift from S. Scherer), ligated to *Eco*RI linkers, and digested with *Eco*RI. The cDNA was separated from excess linkers by Sephacryl S-1000 (Pharmacia) chromatography, ligated into the *Eco*RI site of λgt10, and packaged in vitro. The library contained 1.5×10^6 individual recombinants with an average insert size of 1.4 kb. The insert size was determined by the average of 30 randomly picked recombinants. Actin-hybridizable sequences were detected in 0.1% of the cDNA inserts.

Screening. The cDNA library was plated at a density of 1,000 PFU/150-mm-diameter dish. Three lifts were made from each plate with nylon membranes (ICN Biomedicals), using methods specified by the manufacturer. The first lift of each plate was hybridized with a GFAP cDNA (11) labeled with ^{32}P to identify recombinants with GFAP inserts and prevent their isolation. The second lift was hybridized with ^{32}P-labeled first-strand cDNA synthesized from C57BL/Control poly(A)$^+$ mRNA (16 weeks postinoculation). The third lift was hybridized with ^{32}P-labeled first-strand cDNA synthesized from C57BL/Scrapie poly(A)$^+$ mRNA (16 weeks postinoculation). Plaques that displayed a difference in signal between the two first-strand cDNA probes and no signal with the GFAP probe were cored and replated at a very low density for rescreening. Again, replicate lifts were made and hybridized with the C57BL/Control and C57BL/Scrapie first-strand cDNA probes.

Following the secondary screen, differentially hybridizing recombinants were purified in small quantities using LambdaSorb (Promega), cut with *Eco*RI, and electrophoresed in low-gelling-temperature agarose. The inserts of each recombinant were excised from the gel and labeled with ^{32}P, using the random priming method of Feinberg and Vogelstein (17, 18) for cross-hybridization analysis.

Sequencing. The cDNA inserts were isolated and subcloned into the *Eco*RI site of the pBluescript plasmid (Stratagene). Double-stranded DNA was used for dideoxy sequencing (45), using the T7 Sequenase system from United States Biochemical Corp. and [α-^{35}S]dATP (1,000 Ci/mmol; Amersham). The M13 universal and reverse sequencing primers were used to sequence the ends of the cDNAs. Oligonucleotides were synthesized corresponding to the 3′ end of each sequence obtained, and this process was repeated until both strands of the inserts were completely sequenced.

Northern blot analyses. Poly(A)$^+$ mRNA (500 ng per lane) was size fractionated by formaldehyde gel electrophoresis (32). After electrophoresis, the RNA was transferred and fixed to a nylon membrane (ICN). The blots were hybridized at low stringency (42°C in 30% formamide) because of cross-species sequence diversity. Probes were labeled by nick translation to a specific activity of 10^9 cpm/μg using [α-^{32}P]dCTP (3,000 Ci/mmol; Amersham).

After hybridization, the membranes were washed for 2 h in several changes of 2× SSC (1× SSC is 0.15 M NaCl plus 0.015 M sodium citrate)–0.1% sodium dodecyl sulfate (SDS) at room temperature and then for 5 h in several changes of 3× SSC–0.1% SDS at 50°C. The membranes were sealed in plastic bags and exposed to Kodak XAR-5 film at −70°C using Dupont Cronex Lightning Plus intensifying screens.

After the proper exposure was obtained, the probe was removed by placing the membranes in 25 mM Tris-HCl (pH 7.5)–0.1% SDS at 90 to 95°C for 1 h followed by 0.1% SDS at 65°C for several hours. The membranes were then used for rehybridization.

For relative quantitation of the RNA on the membrane, the blots were hybridized to several control probes. The amount of actin mRNA present was determined by hybridization with a ^{32}P-labeled nick-translated β-actin cDNA. The cDNA library was screened with an actin-specific oligonucleotide. A 1-kb cDNA insert was selected, subcloned, and partially sequenced. This cDNA extends from base 274 to base 1279 of the mouse cytoskeletal mRNA for β-actin (49). Signal intensities were measured by densitometric scanning of the autoradiographs, and the values were normalized to those for actin. To substantiate the use of actin as a control, the blots were also hybridized sequentially to several randomly picked inserts from the cDNA library. The actin and randomly picked cDNA probes gave similar relative signals (data not shown).

For size determination of the mRNAs, 5 μg of the 0.24- to 9.5-kb and the 0.16- to 1.77-kb RNA ladders (Bethesda Research Laboratories) were run in parallel with the poly(A)$^+$ mRNA. After electrophoresis, transfer, and baking

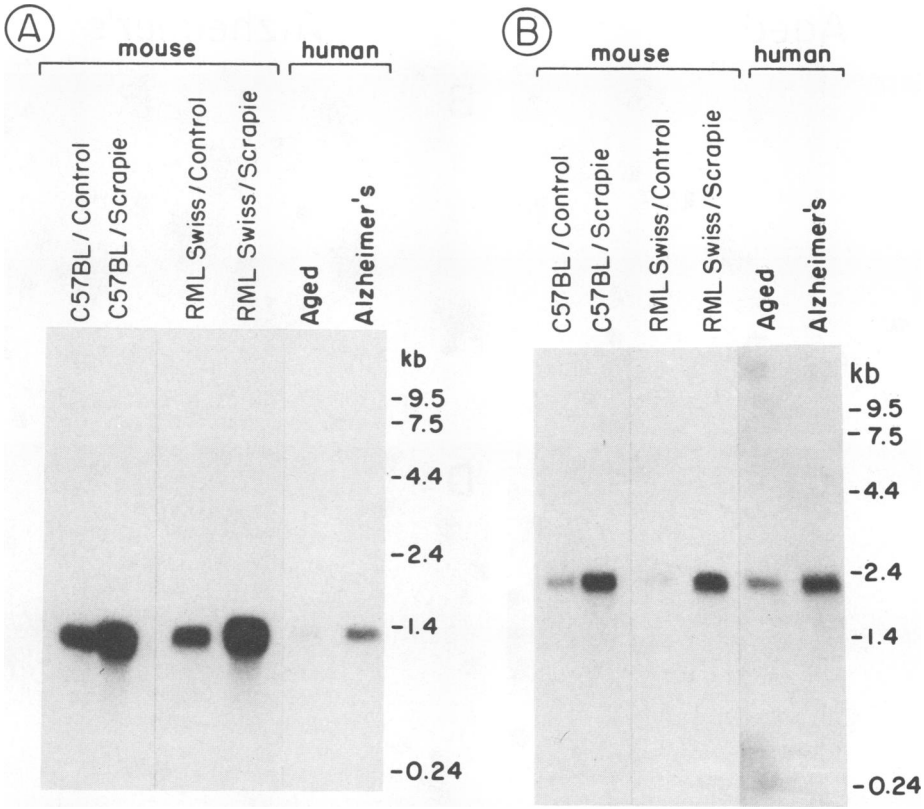

FIG. 1. Northern blot analyses of apoE and CD mRNA in control and diseased brain tissues. The RNA transfer blots contained 500 ng of poly(A)$^+$ RNA isolated from the brains of C57BL/6J mice (16 weeks postinoculation) injected with normal mouse brain homogenate (C57BL/Control) or with brain homogenate of mice infected with the 22L strain of scrapie (C57BL/Scrapie), RNA from RML Swiss mice injected with normal mouse brain homogenate (RML Swiss/Control) or with brain homogenate of mice infected with the Chandler strain of scrapie (RML Swiss/Scrapie), or RNA from the frontal cortex of an elderly patient without clinical or histological evidence of AD (Aged) or with clinical and histological evidence of AD (Alzheimer's). (A) The blots were hybridized with the 1-kb apoE cDNA labeled with ^{32}P to a specific activity of 1.5×10^9 cpm/μg. The mouse lanes were exposed to film for 1 h, and the human lanes were exposed for 15 h at −70°C, using Dupont Cronex Lightning Plus intensifying screens. (B) The blots were hybridized with the 1.5-kb CD cDNA labeled with ^{32}P to a specific activity of 1.5×10^9 cpm/μg. The mouse lanes were exposed to film for 1 h, and the human lanes were exposed for 40 h, using the conditions described for panel A.

of the membrane, the RNA ladder lanes were cut from the membrane and stained with methylene blue as described by Monroy (34).

In situ hybridization. Sections were cut at 8- to 10-μm thicknesses, and in situ hybridizations were performed as described by Brahic and Haase (3). Probes were labeled by nick translation to a specific activity of 10^9 cpm/μg using [α-^{35}S]dATP and [α-^{35}S]dCTP (1,000 Ci/mmol; Amersham). Sections were hybridized with the probes at a concentration of 2×10^8 cpm/ml. After development of the emulsion, the sections were stained with cresyl violet (6).

A number of control experiments were performed. A 1-kb mouse GFAP cDNA probe was used in some experiments to label astrocytes; this cDNA is located within the 3′ untranslated region of the GFAP mRNA (11, 30). RNase control sections were incubated with 300 μg of RNase A per ml and 60 μg of RNase T_1 per ml for 1 h at 37°C prior to acetylation. In addition, a heterologous probe control experiment was also performed. *E. coli* DNA was nick translated and hybridized along with the test probes. No observable hybridization was seen with the RNase or the heterologous probe controls (data not shown).

Immunocytochemistry. Tissue sections were deparaffinized in xylene and placed in 100% ethanol. Endogenous peroxidase activity was blocked by placing the sections in 1% H_2O_2 in methanol for 10 min. The sections were hydrated through graded ethanol, rinsed in phosphate-buffered saline, and incubated for 20 min with normal goat serum. Incubations with the rabbit antisera were performed at 4°C overnight at the following dilutions: anti-rat apoE, 1:200; anti-human GFAP, 1:1,000; anti-rat CD, 1:2,000; and anti-human CD, 1:4,000 (50). This procedure was followed by a biotinylated secondary antibody and an avidin-biotinylated horseradish peroxidase complex (Vector Laboratories). The slides were incubated in freshly prepared substrate (0.05% diaminobenzidine tetrahydrochloride, 0.01% H_2O_2, 50 mM Tris-HCl [pH 7.2]) for 1 to 5 min, rinsed, and stained with cresyl violet.

Control reactions involved substitution of primary antiserum by normal rabbit serum or preimmune serum, and no peroxidase reaction products were observed. Since apoE is present in serum, test reactions were performed by using 0.1% bovine serum albumin as blocking agent in place of the diluted goat serum. The diluted serum was used for subsequent studies because it reduced background staining and produced no observable signal interference.

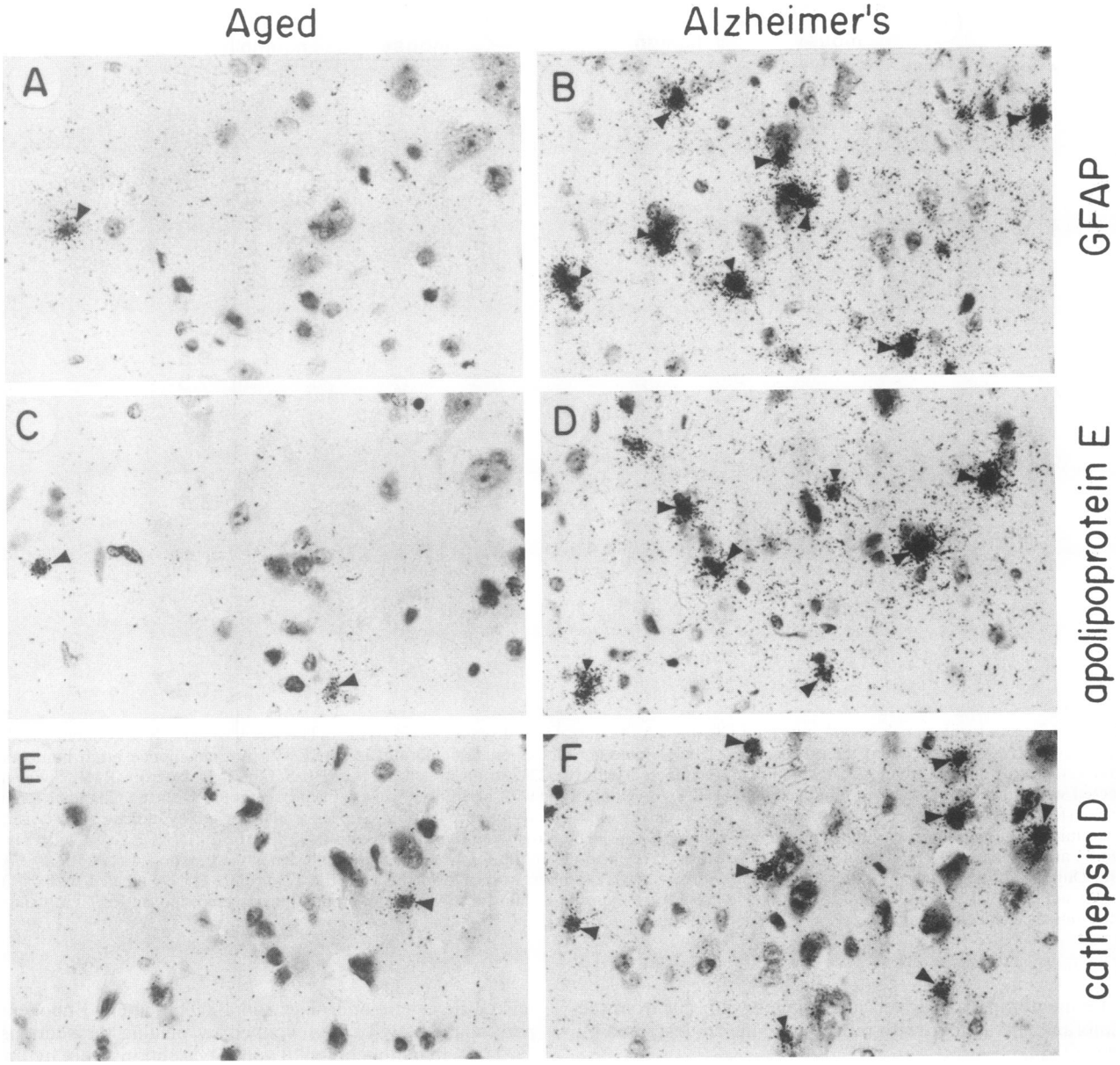

FIG. 2. Localization by in situ hybridization of GFAP, apoE, and CD mRNAs in the cortex of a control and an AD patient. Sections from the frontal cortex of a control brain are shown in the left panels and those from an AD brain are shown in the right panels. Serial sections were hybridized with ^{35}S-labeled GFAP cDNA (A and B), apoE cDNA (C and D), or CD cDNA (E and F). Silver grains representing hybridization signal are visible as black spots. With all three probes, sections from the AD brain (B, D, and F) show a large number of strongly positive astrocytes (arrowheads) compared with the few weakly positive astrocytes (arrowheads) in the control sections (A, C, and E).

Amyloid staining. Amyloid was demonstrated by staining the sections with Congo red, using Puchtler's modification of Benhold's procedure (41, 42). To demonstrate immunoreactive apoE or CD and amyloid in the same sections, the tissues were first immunolabeled as described above. Then, after incubation with the substrate and rinsing in distilled water, the sections were treated with alkali and stained in the alkaline Congo red solution.

Nucleotide sequence accession number. The EMBL accession number of the nucleotide sequence determined in this study is M73490.

RESULTS

Screening and nucleotide sequence analyses. We differentially screened 10,000 recombinants in the scrapie cDNA library and after subsequent rounds of screening and cross-hybridization studies identified two cDNAs corresponding to mRNAs that were increased in scrapie. We subcloned these cDNAs into plasmids, sequenced them, and after a search of the GenBank data base found 99.7% identity between the sequence of one of these cDNAs and that of mouse apoE mRNA (43). This 1-kb cDNA began 74 nucleotides after the initiation codon and ended 13 nucleotides

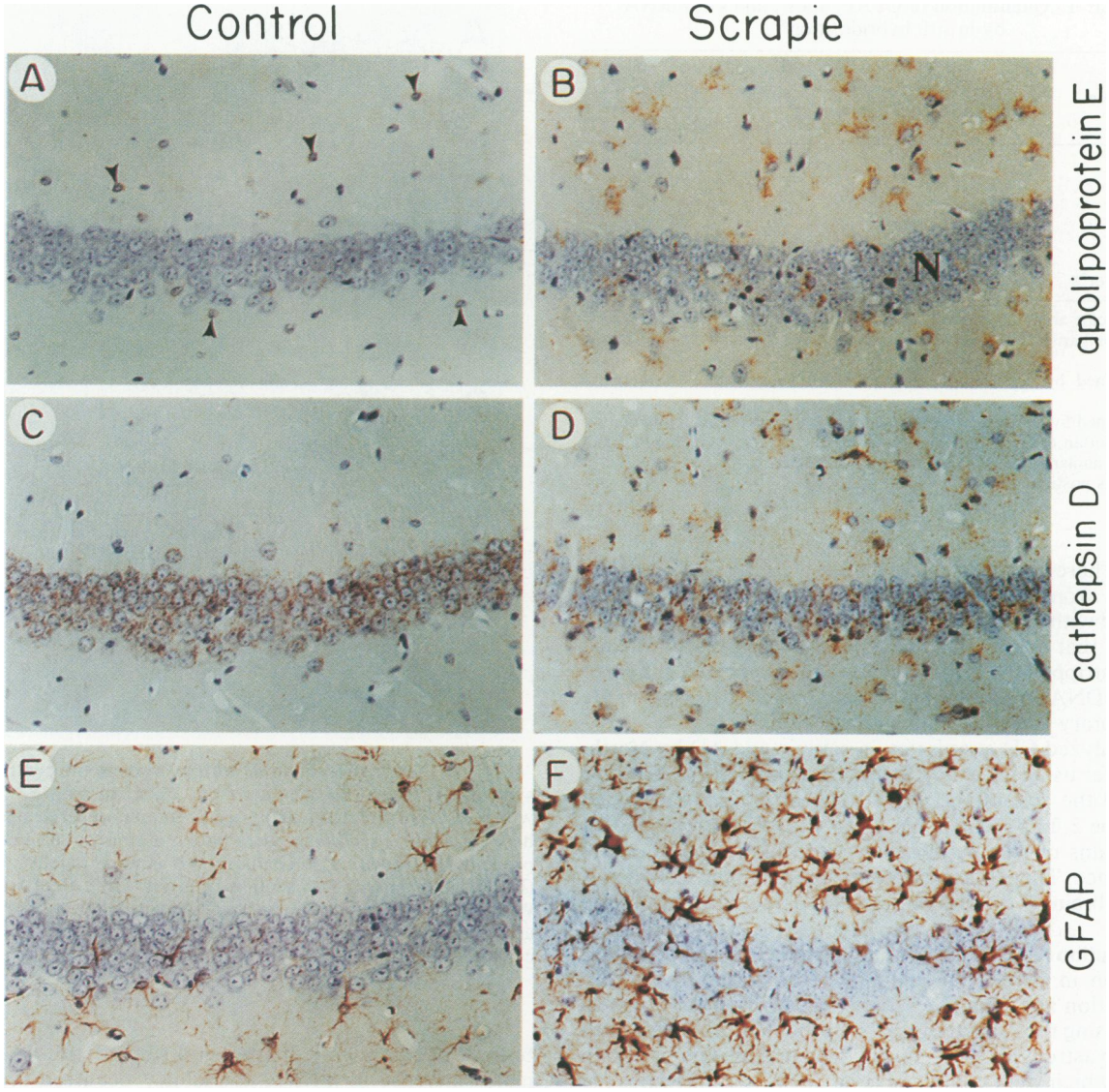

FIG. 3. Localization of GFAP, apoE, and CD in the hippocampus of control and scrapie-infected mice. Sections from control mice (20 weeks postinoculation) are displayed in the left panels, and sections from scrapie-infected mice (20 weeks postinoculation) are in the right panels. Sections were reacted with anti-apoE serum (A and B), anti-CD serum (C and D), or anti-GFAP serum (E and F). Antigen-antibody reaction is represented by a reddish brown precipitate against the purple-blue counterstain. The section from the control mouse reacted with anti-apoE serum (A) shows few weakly positive astrocytes (arrowheads), with the reaction product closely associated with the nucleus, whereas the section from the scrapie-infected mouse (B) shows numerous strongly positive astrocytes on both sides of the neuron layer (N), with immunoreactive apoE extending far into the astrocytic processes. The control section treated with anti-CD serum (C) shows reactivity predominantly in the neuron layer, whereas the section from the scrapie-infected mouse (D) shows strong reactivity, with astrocytes on both sides of the neuron layer and an increase in CD dispersed within the neuropil. The decrease in neuronal staining seen in the scrapie-infected mouse (D) was not a consistent finding. The section from the control animal reacted with anti-GFAP serum (E) shows few weakly positive astrocytes, whereas the section from the infected animal (F) shows an increase in the number, size, and reactivity of astrocytes as well as hypertrophied astrocytic processes.

before the poly(A) tail. Our sequence was different from that of the previously published sequence at three nucleotide positions; two of these differences did not change the deduced amino acid sequence, and the third resulted in the conversion of an aspartic acid to a glutamic acid at amino acid residue 163. Using this same strategy, we found that the second cDNA encoded CD (EC 3.4.23.5). This sequence has been published previously (13; EMBL accession number X53337).

Northern blot analyses. We then examined the expression of the apoE gene in scrapie and AD by Northern transfer, using the 1-kb apoE cDNA insert as a probe (Fig. 1A). We estimated the size of the apoE mRNA in mouse and human brains to be 1.2 kb. This mRNA was threefold more abundant in the brains of scrapie-infected animals (C57BL/Scrapie and RML Swiss/Scrapie) than in the brains of control animals (C57BL/Control and RML Swiss/Control), as determined by densitometric scanning of the autoradio-

TABLE 1. Quantitation of GFAP, apoE, and CD mRNA by in situ hybridization[a]

Brain tissue	No. of astrocytes/field[b]	Amt of RNA hybridized (grains/astrocyte)[c] with:		
		GFAP	apoE	CD
Mouse[d]				
Control	9	8	9	8
Scrapie	20	40	33	38
Human				
Aged	8	14	9	4
Alzheimer's	21	57	55	21

[a] The specific activities of the probes as well as the exposure times varied such that comparisons could only be made between the control and diseased of each set.

[b] Determined by histological analyses of 50 fields within the cerebral cortex.

[c] Determined by averaging the number of grains over 50 randomly chosen astrocytes within the cerebral cortex and subtracting the average number of grains over similar adjacent areas without astrocytes.

[d] 16 weeks postinoculation.

graphs. There was a twofold increase in the apoE mRNA from the frontal cortex of an AD patient (Alzheimer's) compared with that of a nondemented elderly patient (Aged). To verify that equal amounts of RNA were present in each lane, we stripped the blots of probe and rehybridized them to an actin cDNA and several randomly picked inserts from the cDNA library (see Materials and Methods).

We analyzed CD expression in scrapie and AD by Northern transfer using a 1.5-kb CD cDNA as probe (Fig. 1B). We estimated the size of the CD mRNA in mouse and human brain to be 2.2 kb. This mRNA was fivefold more abundant in the brains of scrapie-infected mice than in the brains of control mice. There was a twofold increase in the CD mRNA from the brain of the AD patient compared with that of the control.

Distribution of apoE mRNA and protein. We mapped apoE expression in mouse and human brain tissues by in situ hybridization and immunocytochemistry. By in situ hybridization, using the 1-kb apoE cDNA probe, apoE mRNA was present in astrocytes in the four human and nine mouse brain controls which were examined (Fig. 2C; Fig. 2 illustrates the localization in human brain; identical localization in astrocytes occurred in the mouse brains). Astrocytes were identified by their nuclear morphology and coincident distribution with cells identified as astrocytes by staining adjacent sections with anti-GFAP serum or by hybridization with a GFAP cDNA (Fig. 2A). We did not detect apoE mRNA in neurons, oligodendrocytes, microglia, ependymal cells, or the choroid plexus.

In scrapie and AD, astrocytes are activated and they increase in number, size, and GFAP content (11, 16). In the diseased brains (four human and nine mouse) by in situ hybridization, we found apoE mRNA increased in astrocytes in parallel with the increase in GFAP mRNA in both scrapie and AD (Table 1, Fig. 2A through D). This increase in apoE mRNA was due to an increase in the number of astrocytes as well as to increased expression within individual cells (Table 1).

The product of the estimated three- to sixfold increase of apoE mRNA in individual cells and the twofold increase in the number of astrocytes (Table 1) is greater than the two- to threefold change in mRNA levels determined from Northern blot analysis (Fig. 1A). We attribute this to the effect of population-biased assays. In the Northern blot analysis, both white and gray matter contributed mRNA and the major increase in mRNA abundancy occurred in the gray matter. In in situ hybridization, we estimated maximum increases of apoE mRNA by counting grains over astrocytes in gray matter in regions with extensive pathological alterations.

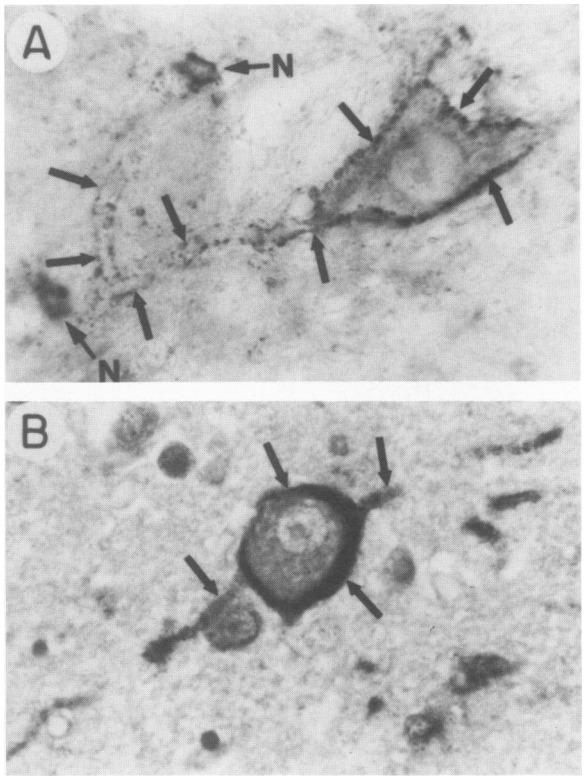

FIG. 4. Association of apoE with neurons in the central nervous system. (A) Brain stem section from a control mouse was reacted with antiserum directed against apoE. Immunoreactive apoE is seen here as a dark precipitate surrounding a neuron cell body and its processes (arrows). Also seen are two immunoreactive astrocytes (N). (B) Cerebral cortex section from an AD patient was reacted with antiserum to apoE. A large neuron is seen with a heavy accumulation of immunoreactive apoE (dark precipitate) around its cell body and associated with its processes (arrows).

In immunocytochemical studies of control brains, we found apoE associated with astrocytes (Fig. 3A). The reaction product was concentrated in the perinuclear region and in processes that terminated on blood vessels and the pial surface. In addition to the reactivity with astrocytes, there was also reaction product associated with the cellular membrane of occasional neurons (Fig. 4A), most evident in the mouse in the posterior portion of the cortex. There were also weakly reactive neurons in the diencephalon, brain stem, and cerebellar medulla. In diseased brains we also documented increased apoE expression within activated astrocytes. We observed a marked increase in apoE associated with astrocytes in scrapie (Fig. 3B) and in AD (data not shown) compared with the controls (Fig. 3A). Using adjacent sections reacted with anti-GFAP serum (Fig. 3E and F), we found that apoE and GFAP expression increased in the same population of cells. Furthermore, immunoreactive apoE extended well into the astrocytic processes in the infected mice (Fig. 3B) in contrast to its perinuclear location

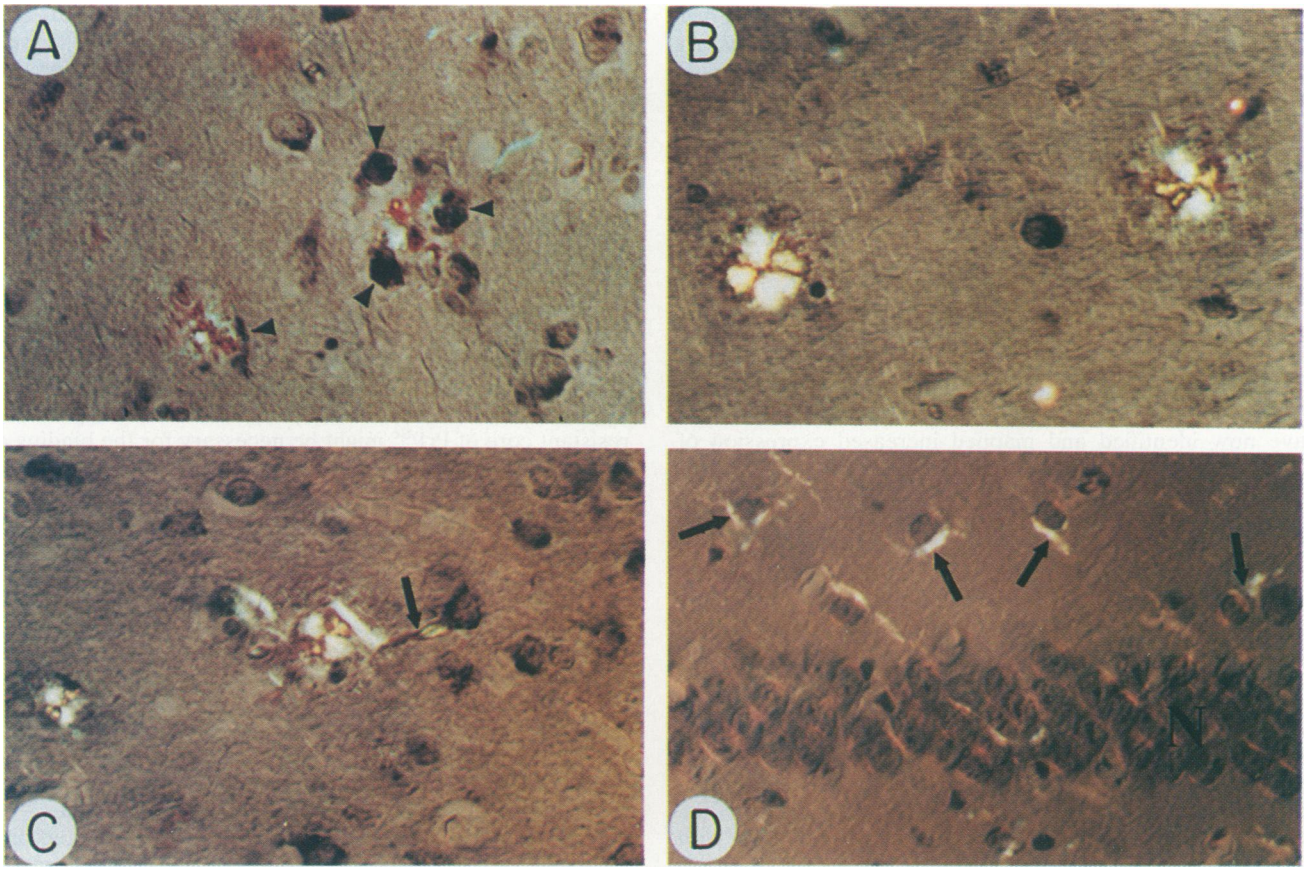

FIG. 5. Close association of CD-positive cells and amyloid plaques in AD. Cerebral cortex sections from AD patients were immunostained for CD (dark brown reaction product) and then stained with Congo red to reveal amyloid (red and/or green plaques and fibrils). CD-positive cells (arrowheads) were often seen surrounding classical amyloid plaques (A) but not compact plaques (B) which are presumed to be mature stages of the former. Panel C shows an amyloid fibril (arrow) extending from a CD-positive cell to an amyloid plaque. Panel D shows a section from the hippocampus of a scrapie-infected mouse (20 weeks postinoculation) stained with Congo red. Amyloid fibrils (arrows) are seen extending from histologically identifiable astrocytes. The neuron layer (N) is indicated.

in the control mice (Fig. 3A). In addition to astrocytes, there was also apoE reaction product associated with neuronal membranes in both scrapie and AD (Fig. 4B) as in the control brains. apoE associated with neurons did not change during scrapie or AD in the amount or distribution of reaction product or in the number of positive cells.

Distribution of CD mRNA and protein. We also mapped CD expression in mouse and human brain tissues by in situ hybridization and immunocytochemistry. By in situ hybridization using the 1.5-kb CD cDNA in control brains, we detected mRNA in a small proportion of astrocytes (Fig. 2E) and in the choroid plexus (data not shown). In AD and in scrapie-infected mice, CD mRNA increased in activated astrocytes (Fig. 2F; Table 1). In the immunocytochemical analyses, we readily detected CD protein in neurons (Fig. 3C) as wells as glia and the choroid plexus. We think that the most likely explanation for detection of this protein in neurons that had little CD mRNA by in situ hybridization is that this mRNA turns over rapidly in neurons, whereas the protein is quite stable. In AD and scrapie, CD increased in activated astrocytes (Fig. 3C and D) in parallel with GFAP (Fig. 3E and F). In scrapie, we observed in addition to accumulations in astrocyte cell bodies, immunoreactive CD within the neuropil (Fig. 3D).

Association of CD with amyloid plaques. To determine the relationship between amyloid plaques and increased gene expression in AD, we combined immunolabeling of apoE or CD with staining of amyloid. We found that CD-positive cells were often present around the periphery of classical plaques (Fig. 5A) but not the compact plaques (Fig. 5B) that are thought to be a more mature stage (53). Furthermore, amyloid fibrils occasionally extended from CD-positive cells to the amyloid plaques (Fig. 5C). Because of the techniques required for this type of analysis, we could not identify the cell type showing CD immunoreactivity. However, in sections stained only for amyloid we found amyloid fibrils primarily associated with astrocytes in scrapie (Fig. 5D) and occasionally associated with astrocytes in AD (data not shown). We did not see any obvious association of apoE-positive astrocytes or neurons with amyloid plaques.

Time course of altered gene expression and lesion development in scrapie. To study the time course of these changes in scrapie, we sacrificed mice every 4 weeks after intracerebral injection of the 22L strain of the scrapie agent or normal mouse brain homogenate. The pathological changes were first apparent at the site of inoculation and then increased in intensity as they progressed from that area throughout the brain. We could detect astrocytosis at 12 weeks postinoculation, and at this time point it was restricted to the cortex and diencephalon. By in situ hybridization and immunocy-

tochemistry, apoE and CD expression was also increased at 12 weeks postinoculation in the cortex and diencephalon. At 16 weeks postinoculation, astrocytosis and increased apoE and CD expression were present throughout the cortex, diencephalon, mesencephalon, and cerebellum. Amyloid and vacuolation were also present at 16 weeks postinoculation to a moderate degree in the cortex and diencephalon and to a lesser degree in the mesencephalon and cerebellum. At the last time point examined (20 weeks postinoculation), there was extensive astrocytosis, increased apoE and CD expression, amyloid, and vacuolation throughout the brain.

DISCUSSION

By combining differential screening of a cDNA library with in situ hybridization and immunocytochemistry, we have now identified and mapped increased expression of three genes to activated astrocytes in the pathological lesions of scrapie and AD (11, 51). The continued success of this experimental approach in defining alterations in gene expression shared by these neurodegenerative diseases supports the hypothesis that convergent pathological mechanisms are involved and provides additional examples of how this approach can provide novel insight into disease processes.

The increase in apoE may represent an attempt by astrocytes to repair or limit damage within the central nervous system. In response to injury to peripheral nerves, macrophages enter the lesions and synthesize and secrete apoE which may function to deliver lipids to neurites and growth cones for membrane biosynthesis (24, 25). In diseases of the central nervous system, such as scrapie and AD, with neuronal injury but without inflammation, astrocytes may assume the role of macrophages in attempting to repair damage (35, 48). Our finding that apoE is either present in astrocytic processes that embrace neurons or is secreted and bound to neuronal membranes (although we cannot exclude synthesis of apoE in neurons, we did not detect transcripts by in situ hybridization) is in accord with such a function for astrocytosis in neurodegenerative diseases.

The increase in CD in astrocytes may represent a convergent pathological pathway in amyloid formation or processing, despite the differences in the amyloid-forming proteins of various diseases. In scrapie, a normal cellular protein, the prion protein, is posttranscriptionally converted to an abnormal isoform (PrP^{Sc}) which aggregates into amyloid fibrils (2, 8, 52). While the normal cellular isoform in the nervous system is predominantly associated with neurons (4, 9, 40), PrP^{Sc} accumulates in astrocytes (12). In AD the major component of amyloid, a 4,200-Da peptide, β-amyloid (19, 33), although unrelated to PrP^{Sc} at the sequence level, has been shown as well to accumulate in astrocytes following chemically induced neuronal damage (46).

The increase in CD, an aspartyl endopeptidase, in astrocytes is compatible with the formation or processing of amyloid, operationally defined by binding of the dye Congo red. In AD, the amyloid precursor protein may be deposited prior to cleavage to the form that binds Congo red, since antisera that recognize epitopes of the β-amyloid precursor outside of the β-amyloid peptide react with non-Congophilic plaques and with a halo around Congophilic plaques, but not the plaque itself (39). Deposition of the precursor may elicit a reaction by astrocytes in which CD attempts to clear the protein and inadvertantly creates the β-amyloid peptide that will aggregate into amyloid and, at high concentrations, acts locally as a neurotoxin (54). The notion that CD produced by astrocytes might be responsible for amyloid formation is supported by our observations that CD-positive cells were frequently found at the periphery of what is thought to be an earlier stage of amyloid formation, the classical plaques of AD, but not around the more mature compact plaques. In addition, amyloid fibrils occasionally extended from CD-positive cells into amyloid plaques (Fig. 5).

In scrapie the relationship of proteolytic cleavage of the precursor protein PrP^{Sc} to formation of amyloid is less clear, but there is evidence that proteolysis of PrP^{Sc} occurs in vivo (23, 26, 44), and proteinase K treatment of scrapie-associated fibrils, whose major component is PrP^{Sc}, enhances staining with Congo red (47). The increase in CD in astrocytes 12 weeks after infection might be in response to the accumulation of the abnormal isoform in astrocytes which begins a month earlier. Subsequent release of the protease-resistant core of PrP^{Sc} might be necessary for the binding of Congo red which results in detection of amyloid 16 weeks after infection. Alternatively, in both scrapie and AD, the increase in CD may be an ongoing response to the deposition of abnormal aggregated proteins that have neurotoxic effects.

Astrocytes were once viewed as passive physical support elements for neurons, but in the last decade, numerous regulatory functions of astrocytes have been discovered (29, 36), and recent evidence suggests that astrocytic networks may constitute pathways for long-range signaling within the brain (7). In this study and in earlier investigations (10), we documented the importance of astrocytes in amyloidogenic neuropathological processes of infectious (scrapie) and unknown etiology (AD). In these conditions, astrocytes "respond" in a concerted and coordinated way. Amyloid proteins may be pathological by-products inadvertently created by astrocytes or may be the stimulus that activates astrocytes to limit damage and repair injury in the central nervous system.

ACKNOWLEDGMENTS

We thank T. L. Innerarity and K. H. Weisgraber (Gladstone Foundation Laboratories) for the anti-apoE serum, L. F. Eng (Stanford University) for the anti-GFAP serum, S. Scherer (University of Minnesota) for the *Eco*RI methylase, J. H. Sung and A. R. Mastri (University of Minnesota) for performing the neuropathological analyses on the human tissues, and T. Leonard for preparation of the figures.

This work was supported by a grant from the National Institutes of Health (NS23446).

REFERENCES

1. **Aviv, H., and P. Leder.** 1972. Purification of biologically active globin messenger RNA by chromatography on oligothymidylic acid-cellulose. Proc. Natl. Acad. Sci. USA **69**:1408–1412.
2. **Bendheim, P. E., R. A. Barry, S. J. DeArmond, D. P. Stites, and S. B. Prusiner.** 1984. Antibodies to a scrapie prion protein. Nature (London) **310**:418–421.
3. **Brahic, M., and A. T. Haase.** 1978. Detection of viral sequences of low reiteration frequency by in situ hybridization. Proc. Natl. Acad. Sci. USA **78**:6125–6129.
4. **Bruce, M. E., P. A. McBride, and C. F. Parquhar.** 1989. Precise targeting of the pathology of the sialoglycoprotein, PrP, and vacuolar degeneration in mouse scrapie. Neurosci. Lett. **102**: 1–6.
5. **Chirgwin, J. M., A. E. Przybyla, R. J. MacDonald, and W. J. Rutter.** 1979. Isolation of biologically active ribonucleic acid from sources enriched in ribonuclease. Biochemistry **18**:5294–5299.
6. **Clark, G. (ed.).** 1981. Staining procedures, 4th ed. The Williams & Wilkins Co., Baltimore.

7. **Cornell-Bell, A. H., S. M. Finkbeiner, M. S. Cooper, and S. J. Smith.** 1990. Glutamate induces calcium waves in cultured astrocytes: long-range glial signaling. Science **247**:470–473.
8. **DeArmond, S. J., M. P. McKinley, R. A. Barry, M. B. Braunfeld, J. R. McCulloch, and S. B. Prusiner.** 1985. Identification of prion amyloid filaments in scrapie-infected brain. Cell **41**:221–235.
9. **DeArmond, S. J., W. C. Mobley, D. L. DeMott, R. A. Barry, J. H. Beckstead, and S. B. Prusiner.** 1987. Changes in the localization of brain prion proteins during scrapie infection. Neurology **37**:1271–1280.
10. **Diedrich, J., S. Wietgrefe, A. Haase, J. Duguid, and R. Carp.** Identifying and mapping changes in gene expression involved in the neuropathology of scrapie and AD. Curr. Top. Microbiol. Immunol., in press.
11. **Diedrich, J., S. Wietgrefe, M. Zupancic, K. Staskus, E. Retzel, A. T. Haase, and R. Race.** 1987. The molecular pathogenesis of astrogliosis in scrapie and Alzheimer's disease. Microb. Pathog. **2**:435–442.

11a. **Diedrich, J. F.** Unpublished data.

12. **Diedrich, J. F., P. E. Bendheim, Y. S. Kim, R. I. Carp, and A. T. Haase.** 1991. Scrapie associated prion protein accumulates in astrocytes during scrapie infection. Proc. Natl. Acad. Sci. USA **88**:375–379.
13. **Diedrich, J. F., K. A. Staskus, E. F. Retzel, and A. T. Haase.** 1990. Nucleotide sequence of a cDNA encoding mouse cathepsin D. Nucleic Acids Res. **18**:7184.
14. **Duguid, J. R., C. W. Bohmont, N. Liu, and W. W. Tourtellotte.** 1989. Changes in brain gene expression shared by scrapie and Alzheimer's disease. Proc. Natl. Acad. Sci. USA **86**:7260–7264.
15. **Duguid, J. R., R. G. Rohwer, and B. Seed.** 1988. Isolation of cDNAs of scrapie-modulated RNAs by subtractive hybridization of a cDNA library. Proc. Natl. Acad. Sci. USA **86**:5738–5742.
16. **Eng, L. F.** 1988. Regulation of glial intermediate filaments in astrogliosis, p. 79–90. *In* M. D. Norenberg, L. Hertz, and A. Schousboe (ed.), The biochemical pathology of astrocytes. A. R. Liss, New York.
17. **Feinberg, A. P., and B. Vogelstein.** 1983. A technique for radiolabeling DNA restriction endonuclease fragments to high specific activity. Anal. Biochem. **132**:6–13.
18. **Feinberg, A. P., and B. Vogelstein.** 1984. A technique for radiolabeling DNA restriction endonuclease fragments to high specific activity. Addendum. Anal. Biochem. **137**:266–267.
19. **Glenner, G. G., and C. W. Wong.** 1984. Alzheimer's disease and Down's syndrome: sharing of a unique cerebrovasular amyloid fibril protein. Biochem. Biophys. Res. Commun. **122**:1131–1135.
20. **Gubler, U., and B. J. Hoffman.** 1983. A simple and very effective method for generating cDNA libraries. Gene **25**:263–269.
21. **Haase, A. T., E. Lewis, S. Wietgrefe, M. Zupancic, J. Diedrich, H. Minnigan, and M. J. Ball.** 1986. Speculations on the role of transmissible agents in the pathogenesis of Alzheimer's disease. Canad. J. Neurol. Sci. **13**:449–451.
22. **Hadlow, W. J., S. B. Prusiner, R. C. Kennedy, and R. E. Race.** 1980. Brain tissue from person dying of Creutzfeldt-Jakob disease causes scrapie-like encephalopathy in goats. Ann. Neurol. **8**:628–632.
23. **Hope, J., G. Multhaup, L. J. D. Reekie, R. H. Kimberlin, and K. Beyreuther.** 1988. Molecular pathology of scrapie-associated fibril protein (PrP) in mouse brain affected by the ME7 strain of scrapie. Eur. J. Biochem. **172**:271–277.
24. **Ignatius, M. J., P. J. Gebicke-Haerter, R. E. Pitas, and E. M. Shooter.** 1987. Apolipoprotein E in nerve injury and repair. Prog. Brain Res. **71**:177–184.
25. **Ignatius, M. J., P. J. Gebicke-Harter, J. H. P. Skene, J. W. Schilling, K. H. Weisgraber, R. W. Mahley, and E. M. Shooter.** 1986. Expression of apolipoprotein E during nerve degeneration and regeneration. Proc. Natl. Acad. Sci. USA **83**:1125–1129.
26. **Kascsak, R. J., R. Rubenstein, P. A. Merz, R. I. Carp, H. M. Wisniewski, and H. Diringer.** 1985. Biochemical differences among scrapie-associated fibrils support the biological diversity of scrapie agents. J. Gen. Virol. **66**:1715–1722.
27. **Khachaturian, Z. S.** 1985. Diagnosis of Alzheimer's disease. Arch. Neurol. **42**:1097–1105.
28. **Kim, Y. S., R. I. Carp, S. M. Callahan, and H. W. Wisniewski.** 1987. Incubation periods and survival times for mice injected stereotaxically with three scrapie strains in different brain regions. J. Gen. Virol. **68**:695–702.
29. **Kimelberg, H. K. (ed.).** 1988. Glial cell receptors. Raven Press, New York.
30. **Lewis, S. A., J. M. Balcarek, V. Krek, M. Shelanski, and N. J. Cowan.** 1984. Sequence of a cDNA clone encoding mouse glial fibrillary acidic protein: structural conservation of intermediate filaments. Proc. Natl. Acad. Sci. USA **81**:2743–2746.
31. **Liberski, P. P., R. Yanagihara, C. J. Gibbs, Jr., and D. C. Gajdusek.** 1989. Neuroaxonal dystrophy: an ultrastructural link between subacute spongiform virus encephalopathies and Alzheimer's disease, p. 549–557. *In* K. Iqbal, H. M. Wisniewski, and B. Winblad (ed.), Alzheimer's disease and related disorders. A. R. Liss, New York.
32. **Maniatis, T., E. F. Fritsch, and J. Sambrook.** 1982. Molecular cloning: a laboratory manual. Cold Spring Harbor Laboratory, New York.
33. **Masters, C. L., G. Simms, N. A. Weinman, G. Multhaup, B. L. McDonald, and K. Beyreuther.** 1985. Amyloid plaque core protein in Alzheimer disease and Down syndrome. Proc. Natl. Acad. Sci. USA **82**:4245–4249.
34. **Monroy, A. F.** 1988. Staining immobilized RNA ladder. BRL FOCUS **10(1)**:14.
35. **Muller, H. W., P. J. Gebicke-Harter, D. H. Hangen, and E. M. Shooter.** 1985. A specific 37,000-dalton protein that accumulates in regenerating but not in nonregenerating mammalian nerves. Science **228**:499–501.
36. **Norenberg, M. D., L. Hertz, and A. Schousboe (ed.).** 1988. Biochemical pathology of astrocytes. A. R. Liss, New York.
37. **Okayama, H., and P. Berg.** 1982. High-efficiency cloning of full-length cDNA. Mol. Cell. Biol. **2**:161–170.
38. **Panter, S. S., J. D. McSwigan, J. R. Sheppard, C. R. Emory, and W. H. Frey II.** 1985. Glial fibrillary acidic protein and Alzheimer's disease. Neurochem. Res. **10**:1567–1576.
39. **Perry, G., S. Siedlak, P. Mulvihill, M. Kancherla, M. Mijares, M. Kawai, P. Gambetti, S. Sharma, L. Maggiora, J. Cornette, T. Lobl, and B. Greenberg.** 1989. Immunolocalization of the amyloid precursor protein within the senile plaque, p. 1021–1025. *In* K. Iqbal, H. M. Wisniewski, and B. Winblad (ed.), Alzheimer's disease and related disorders. A. R. Liss, New York.
40. **Piccardo, P., J. Sagar, M. Ceroni, D. C. Gajdusek, and C. J. Gibbs, Jr.** 1990. Immunohistochemical localization of prion protein in spongiform encephalopathies and normal brain tissue. Neurology **40**:518–522.
41. **Puchtler, H., and F. Sweat.** 1965. Congo red as a stain for fluorescence microscopy of amyloid. J. Histochem. **13**:693–694.
42. **Puchtler, H., F. Sweat, and M. Levine.** 1962. On the binding of Congo red by amyloid. J. Histochem. **10**:355–364.
43. **Rajavashisth, T. B., J. S. Kaptein, K. L. Reue, and A. J. Lusis.** 1985. Evolution of apolipoprotein E: mouse sequence and evidence for an 11-nucleotide ancestral unit. Proc. Natl. Acad. Sci. USA **82**:8085–8089.
44. **Rubenstein, R., R. J. Kascsak, P. A. Merz, M. C. Papini, R. I. Carp, N. K. Robakis, and H. M. Wisniewski.** 1986. Detection of scrapie-associated fibril (SAF) proteins using anti-SAF antibody in non-purified tissue preparations. J. Gen. Virol. **67**:671–681.
45. **Sanger, F., S. Nicklen, and A. R. Coulson.** 1977. DNA sequencing with chain-terminating inhibitors. Proc. Natl. Acad. Sci. USA **74**:5463–5467.
46. **Siman, R., J. P. Card, R. B. Nelson, and L. G. Davis.** 1989. Expression of β-amyloid precursor protein in reactive astrocytes following neuronal damage. Neuron **3**:275–285.
47. **Somerville, R. A., L. A. Ritchie, and P. H. Gibson.** 1989. Structural and biochemical evidence that scrapie-associated fibrils assemble in vivo. J. Gen. Virol. **70**:25–35.
48. **Stoll, S., and H. W. Muller.** 1986. Macrophages in the peripheral nervous system and astroglia in the central nervous system of rat commonly express apolipoprotein E during development but differ in their response to injury. Neurosci. Lett. **72**:233–

238.
49. **Tokunaga, K., H. Taniguchi, K. Yoda, M. Shimizu, and S. Sakiyama.** 1986. Nucleotide sequence of a full-length cDNA for mouse cytoskeletal β-actin mRNA. Nucleic Acids Res. **14**:2829.
50. **Whitaker, J. N.** 1981. Comparative chemical, enzymatic and immunochemical features of brain cathepsin D. Comp. Biochem. Physiol. **63B**:215–220.
51. **Wietgrefe, S., M. Zupancic, A. Haase, B. Cheseboro, R. Race, W. Frey II, T. Rustan, and R. L. Friedman.** 1985. Cloning of a gene whose expression is increased in scrapie and in senile plaques in human brain. Science **230**:1177–1179.
52. **Wiley, C. A., P. G. Burrola, M. J. Buchmeier, M. K. Wooddell, R. A. Barry, S. B. Prusiner, and P. W. Lampert.** 1987. Immunogold localization of prion filaments in scrapie-infected hamster brains. Lab. Invest. **57**:646–656.
53. **Wisniewski, H. M., and R. D. Terry.** 1973. Reexamination of the pathogenesis of the senile plaque, p. 1–26. *In* H. M. Zimmerman (ed.), Progress in neuropathology, vol. 2. Grune & Stratton, New York.
54. **Yankner, B. A., L. K. Duffy, and D. A. Kirschner.** 1990. Neurotrophic and neurotoxic effects of amyloid β protein: reversal by tachykinin neuropeptides. Science **250**:279–282.